



## Study and Simulation of the Thrust Vectoring in Supersonic Nozzles

Kbab Hakim<sup>1,\*</sup>, Hamitouche Toufik<sup>1</sup>, Mouloudj Y.<sup>1</sup>

<sup>1</sup> Université de Blida1, Aeronautics and Space Studies Institute, Aeronautical Sciences Laboratory, BP270 Route de Soumàa, Blida, Algeria

### ARTICLE INFO

#### Article history:

Received 18 November 2021

Received in revised form 20 January 2022

Accepted 23 January 2022

Available online 1 March 2022

#### Keywords:

CD Nozzle; TVC; SVC; NPR; CFD; SPR

### ABSTRACT

The present study aims to numerically simulate the thrust vectoring by secondary injection. The analysis of flow for this study was done using ANSYS Fluent. The kw-sst turbulence model was used. The baseline solver was selected as a double-precision Density-based coupled solve with implicit time integration. Least squares cell-based spatial discretization in which the solution was assumed to vary linearly was used and a second-order upwind scheme is used for interpolating the values of pressure, momentum, turbulent kinetic energy, specific dissipation rate, and energy. The computational analysis was conducted under study conditions. The initialization for the steady-state problem was done using full multigrid (FMG) initialization to get the initial solution and the boundary was provided to get the reference value. The results of the study with and without fluid injection are presented in terms of pressure, angle of deflection, and efficiency. These results are then compared with those obtained numerically or experimentally by other authors. This comparison was very interesting and the results were very close, the error was only 5%.

## 1. Introduction

The classical method of deflecting the jet is the "mechanical" method, based on the use of ailerons and moving parts installed at the divergent nozzle. These methods are efficient but expensive. Several disadvantages are also attributed to this type of device. A mechanically orientable nozzle is twice as heavy as a geometrically orientable nozzle as a nozzle with fixed geometry [1,2].

Movable ailerons require a mechanical actuator, whose weights add to that of the engine and increase the complexity of the nozzle and maintenance costs. An alternative to mechanical methods is to deflect the jet by applying a fluid injection directly into the thrust element (usually the nozzles) to obtain a deflection of its momentum. This method is based on concepts originally developed for missile control by lateral jet injection [2,3]. In this injection, the pressure distribution on the walls of the nozzle is changed and the balance of forces is modified.

The advantage of this mode of vectoring is that it does not require any moving mechanical parts other than valves to control the injected fluid. In this case, all the problems associated with moving

\* Corresponding author.

E-mail address: [k71.hakim@gmail.com](mailto:k71.hakim@gmail.com)

<https://doi.org/10.37934/arfmts.93.1.1324>

ailerons are eliminated. However, fluid vectoring has some disadvantages, such as the delicate installation of injection slots, especially in axisymmetric nozzles, and the flow rate of the injected gas, which is generally extracted from the primary flow, which reduces the maximum thrust of the engine at the time of vector. Several principles can be used to vectorize a supersonic nozzle by fluid injection such as Shock Vector Control (SVC), control by sonic line deformation (Throat Skewing), and counter-current mixing layer control [3].

The first studies on thrust vectoring date back to the 1960s [4,5]. The devices studied at the time include mechanisms. These mechanisms are effective, but their disadvantage is the increased weight of the engine and the additional maintenance costs due to the complex systems used by these mechanisms.

During the 1970s, studies concerned non-axisymmetric nozzles: like the two-dimensional convergent-divergent CD-2D, SERN-type nozzles (single-expansion-ramp nozzles) for their ability to adapt to the thrust vectoring [6]. Multiaxis mechanical thrust vectoring was also studied in the 1980s by Gallaway and Osborn [7]. The study of fluid injection to deflect thrust was undertaken in the 1990s [8-11]. First, divergent slots were installed to create asymmetric pressure fields. Several techniques were subsequently tested. The three most used fluidic techniques are injection near the throat (deformation of the sonic line), injection into the diverging SVC (Shock Vector Control), and control by counterflow mixing layer [10-13,16-17]. The studies were carried out on plane nozzles. Many authors then became interested in axisymmetric nozzles. An experimental and numerical study in a CD-2D planar convergent-divergent nozzle was carried out by Waithe and Deere [17], this work highlighted the effects of several parameters influencing the fluidic injection.

In 2014, an approach by Deng *et al.*, [18] was undertaken to see the effect of this method for shock wave control, an analytical model was established to study the height of penetration and pressure distribution for the injector. The effect of chemical reactions on fluidic thrust vectoring of an axisymmetric nozzle was studied by Chouicha *et al.*, [19]. Hakim *et al.*, [20] studied the fluidic injection in a conical nozzle using the mathematical model proposed by Spaid and Zukoski [21], a model based on the calculation of the effective height of the obstacle equivalent to the injected jet and the efficiency of the secondary injection has been demonstrated. A numerical study of the flow in a linear aerospike nozzle was carried out by Ferlauto *et al.*, [22]. a differential throttling and thrust vectoring were investigated using the Reynolds averaged Navier-Stokes equations. The performance of the thrust vectoring was evaluated in terms of lateral force generation.

The effectiveness of the fluidic thrust vectoring was studied by varying the secondary flow mass flow rate and the location of the injection. Emelyanov *et al.*, [23] were interested in the optimal design of the thrust vector control system of solid rocket motors (SRM) considering a slack flow in the nozzle. The turbulent flow of a viscous compressible gas in the main nozzle and injection system is simulated using the Reynolds Averaged Navier-Standard (RANS) method and the shear stress transport (SST) turbulence model. In the study by Xue *et al.*, [24], they investigated the control effects of fluidic thrust vector technology for low-speed aircraft at high altitude/low density and low altitude/high density using the FLUENT software S-A model to simulate the flow field inside and outside the nozzle with varying control surface parameters. They obtained the relationship between the area of the control surface and the deflection effect of the main flow for different altitudes. It was found that the fluidic thrust vector nozzle can effectively control the internal flow on the ground and at high altitude/low density and the deflection angle of the mainstream can be continuously adjusted.

Chandra Sekar *et al.*, [25] conducted an experimental study to evaluate the performance of a fluidic thrust vector convergent nozzle. They found that the thrust coefficient depends on the pressure ratio (NPR) of the primary nozzle and the mass ratio of the primary and secondary

streams. The vector angle depends only on the momentum ratio or mass ratio and is independent of the NPR. It is observed that the injection of the secondary jet increases the magnitude of the net thrust by reducing the effective flow area while reducing the thrust coefficient.

In the study by Song *et al.*, [26], a new concept of a hybrid throat control (TC) nozzle has been proposed to improve the efficiency of neck surface control using a rotary valve with secondary injection. The flow mechanism of the hybrid TC nozzle and the effect of aerodynamic and geometric parameters on the nozzle performance were numerically investigated. Then, the approximate model characterizing the hybrid TC nozzle was established and used to analyze the coupling effect between the parameters and optimize the combination of the parameters.

In the study by Chen and Liao [27], the authors studied the performance of thrust vectoring with secondary injection in a convergent-divergent nozzle. Analytical modeling was performed to determine the location and angle of the shock, providing a guideline for the design and performance of the system. Next, a numerical simulation was performed to understand the effects of injection pressure, injection location, injection angle, and injector on thrust vector performance. And it was found that hydrogen peroxide ( $H_2O_2$ ) can be more effective than air in producing lateral loads

## 2. Computational Methodology

### 2.1 Governing Equations

For a compressible, viscous and assumed perfect fluid, the fundamental equations of flow can be given by the following equation of conservation:

i. Mass equation:

$$\frac{d\rho}{dt} + \frac{d}{dx_j} (\rho u_j) = 0$$

Where  $\rho$  is the density of the fluid and  $u_j$  is the  $j$  component of the velocity vector.

ii. Momentum equation:

$$\frac{d}{dt} (\rho u_i) + \frac{d}{dx_j} (\rho u_i u_j) = \frac{d}{dx_j} (-p \delta_{ij} + \tau_{ij})$$

Where  $p$  is the static pressure,  $\delta_{ij}$  is the Kronecker tensor and  $\tau_{ij}$  the viscous constraints tensor.

iii. Energy equation:

$$\frac{d}{dt} (\rho E_t) + \frac{d}{dx_j} (u_j (\rho E_t + p)) = \frac{d q_j}{dx_j} + \frac{d}{dx_j} (u_i \tau_{ij})$$

Where  $q_j$  is the heat flux in direction  $j$ .

iv. Total energy:

The total energy per unit of mass is defined by the following equation as a function of the internal energy and the kinetic energy:

$$E_t = e + \frac{1}{2} u_k u_k$$

We must also add the equation of state of the perfect gas:

$$P = \rho r T$$

$r$  is the perfect gas constant.

## 2.2 Turbulence Model

Due to the complexity of the flow, the choice of the turbulence model is always a very delicate point when using CFD codes. However, classical RANS models, such as  $k-\epsilon$ ,  $k-\omega$  and  $k-\omega$  SST are widely used and give good results in practice for internal flows. Several criteria have an important influence on the choice of a turbulence model such as the physical nature of the problem, the quality of the expected results and the computational power. In reference of Hakim *et al.*, [20], two turbulence models were tested ( $k-\epsilon$ ,  $k-\omega$  SST) for NPR=3. The chosen model ( $k-\omega$ ) was selected because it adequately reproduces the separation zone compared to the experimental one [16].

## 2.3 Mesh Sensitivity

In our calculations, we will use structured meshes based on quadrilaterals. This type of mesh generally offers a satisfactory numerical resolution. It also allows a homogeneous refinement near the walls to resolve the laminar sublayer of the turbulent boundary layer. It is described generally by using the reduced variable  $y^+$  that defines the height of the first mesh next to the wall [3]. The mesh is composed of several zones. The first one represents the inside of the nozzle with the most cells. The second covers the outer field downstream of the nozzle. The third and fourth zones are respectively at the top and bottom of the nozzle, while the fifth represents the injector. Mesh refinement is also taken into account on the inner walls of the injector to simulate better the boundary layers of the injector. To study the meshing sensitivity, two structured meshes with different cell densities were tested. Mesh A constructed of 48740 cells. Mesh B was composed of 44750 cells. The Figure 1 shows the pressure evolution along the wall for an NPR equal to 5 for both meshes and we note that the variation in the number of cells did not affect the solution. Meshes C generated with 155760 cells. Figure 2 shows the pressure distribution along with the nozzle divergent for NPR= and SPR=0.7 with  $k-\omega$  as the turbulence model. We note that this evolution detected for meshes A and C is similar. Mesh B predicts a separation point upstream of meshes B and C. The resulting interaction zone (which is longer) produces a large deflection than meshes A and C. The meshes A and C results are closer to the NASA experiment results. Given the convergence time taken by mesh C, we chose mesh A. Our choice is a compromise between a mesh closer to the solution and the computation time. It is the same conclusion from reference by Hakim *et al.*, [20].

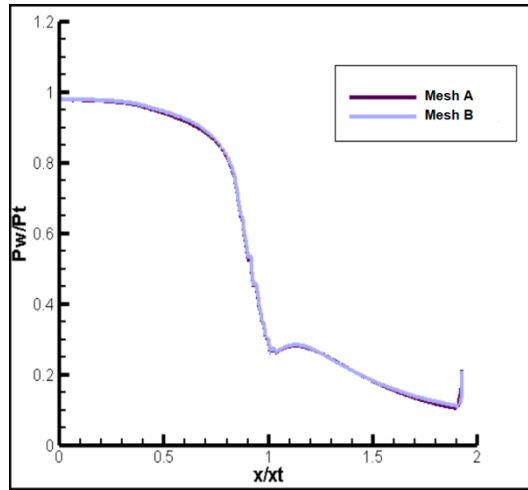


**Fig. 1.** Pressure distribution along the nozzle for different meshes at NPR = 5

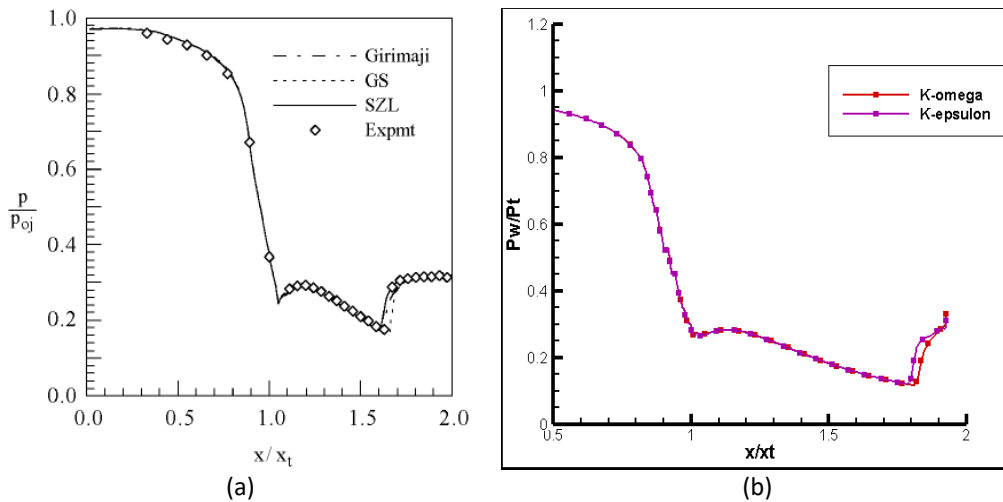


**Fig. 2.** Influence of the turbulence model NPR = 3, (a) Hunter [28], (b) Our calculations

### 3. Application on the TIC Nozzle

The simulated nozzle is a 2D convergent-divergent nozzle with a section ratio of 2.43 and an exit Mach number of 3.5. The length of the divergent part is  $L=0.086\text{m}$ . The injection point is  $X_j/L=0.882$ . The width of the slot is 2.9 mm. The numerical calculations are performed for a stationary turbulent flow. The inlet temperatures of the nozzle and the injectors are  $300\text{ k}^\circ$  and  $243\text{ k}$  respectively and the pressure is 3 bars. Both inlets are considered subsonic with a Mach number of 0.1. The outlet pressure and temperature are 0.08 bar and  $300\text{ k}^\circ$  respectively.

#### 3.1 Effects of NPR

The Figure 3 to 6 below represent the contours of the iso-Mach and the pressure distribution along the walls of the TIC nozzle, for different NPRs (5 to 30).

A separation of the boundary layer was observed at the position  $x / x_t = 0.57$ . An overpressure then appears downstream of the point of impact. This can significantly affect the efficiency of the thrust vectoring.

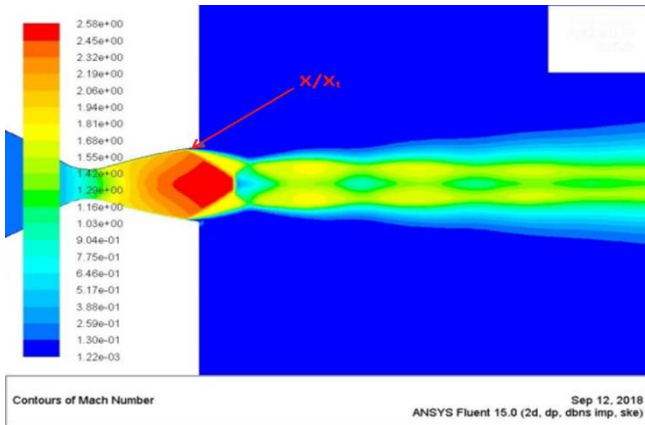


Fig. 3. Iso-Mach and pressure distribution, NPR = 5

We notice that the displacement of the shock to the nozzle's lips and the exit Mach number is equal to 2.63.

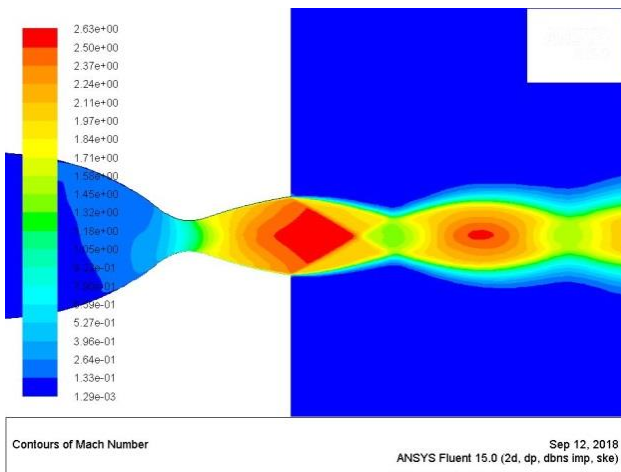


Fig. 4. Iso-Mach and pressure distribution, NPR=7.5

For an NPR = 10 the shock has moved downstream and the number of Mach at the exit becomes 2.66.

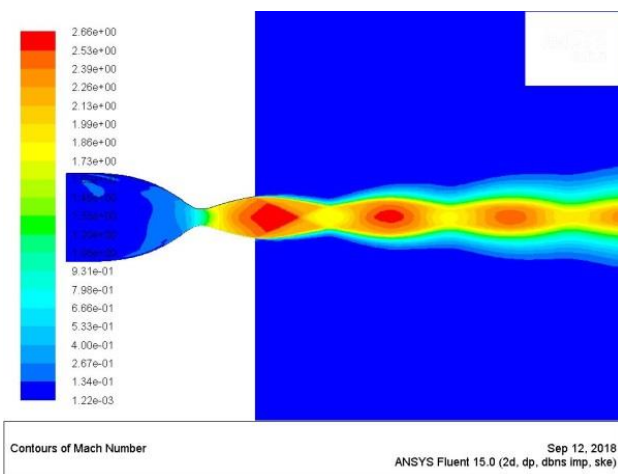
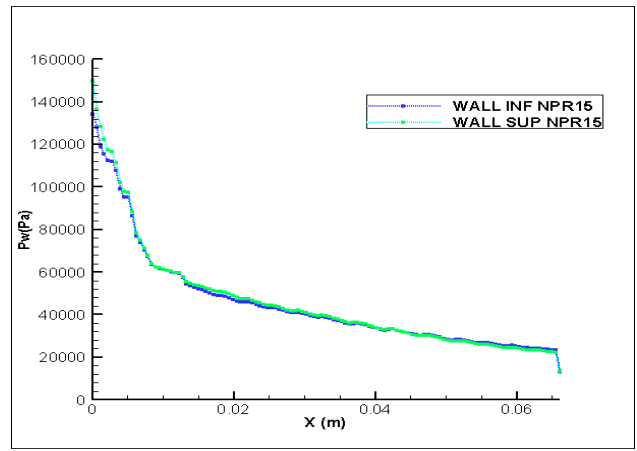
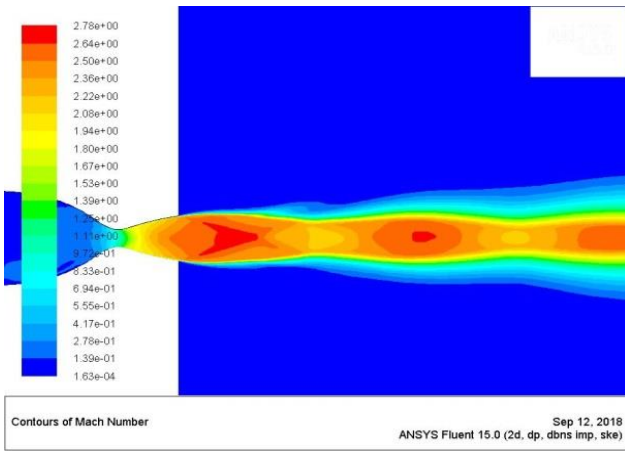
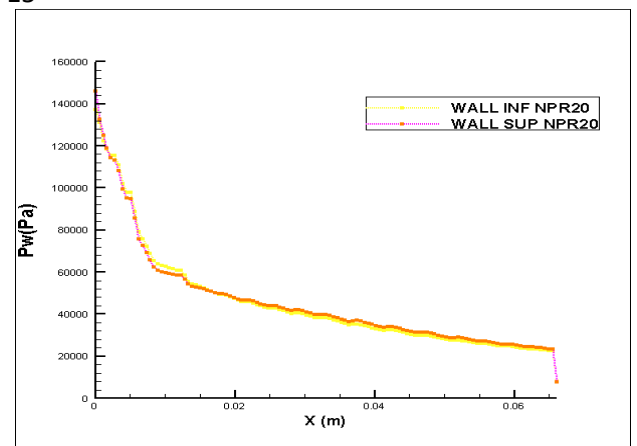
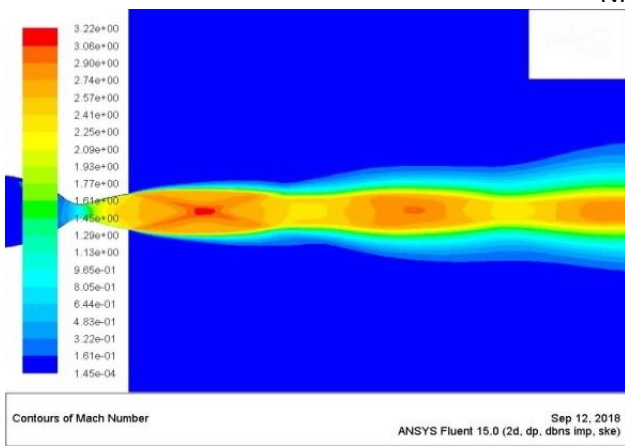


Fig. 5. Iso-Mach and pressure distribution, NPR=10

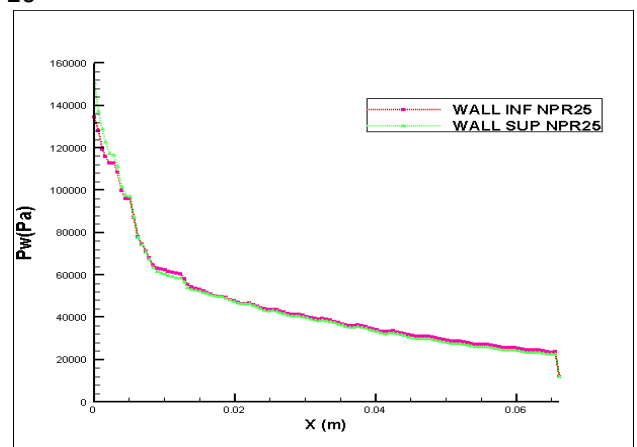
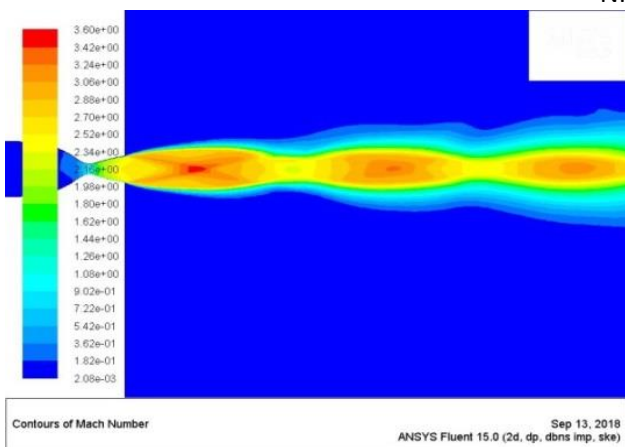
For NPR's greater than 15, we see that the position of the Mach disk moves along the axis of the nozzle. The separation obtained for each NPR is free. This remark is reflected in the pressure plates, which remain constant until the outlet of the nozzle, i.e., no reattachment points.



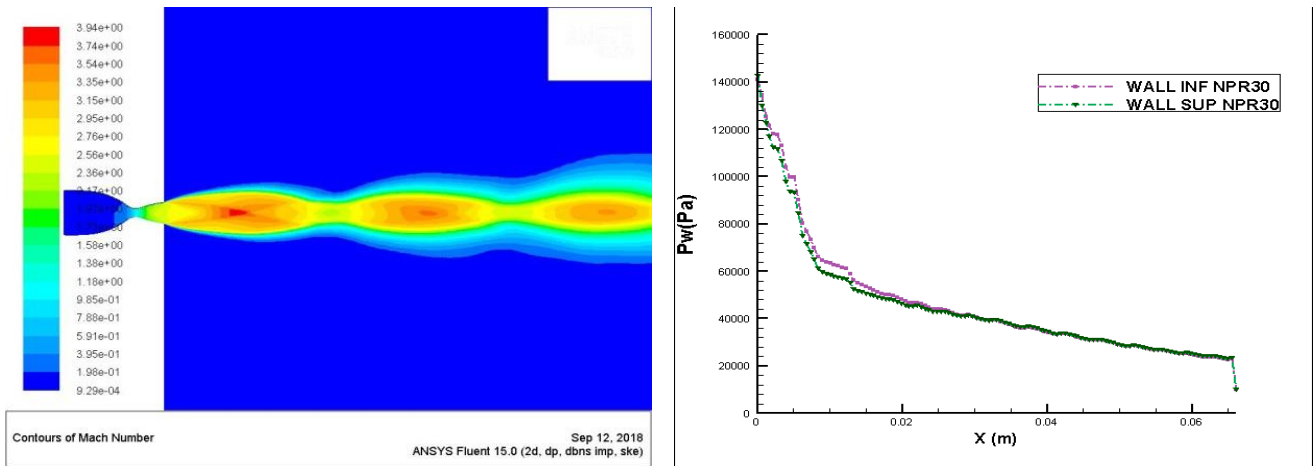
NPR=15



NPR=20



NPR=25



NPR=30  
**Fig. 6.** Iso-Mach and pressure distribution NPR (15, 20, 25, 27, 30)

Indeed, for a pressure rate ranging from 5 to 15, the ambient pressure is greater than the outlet pressure of the nozzle., in this case, the flow is over-expanded with separation until the value of NPR = 15, where the flow becomes suitable ( $P_e = P_a$ ). Above this value, the flow regime is under-expanded, and the outlet pressure is greater than ambient pressure. The pressure distribution on the top and bottom walls of the TIC nozzle is almost identical, see Figure 7 below.

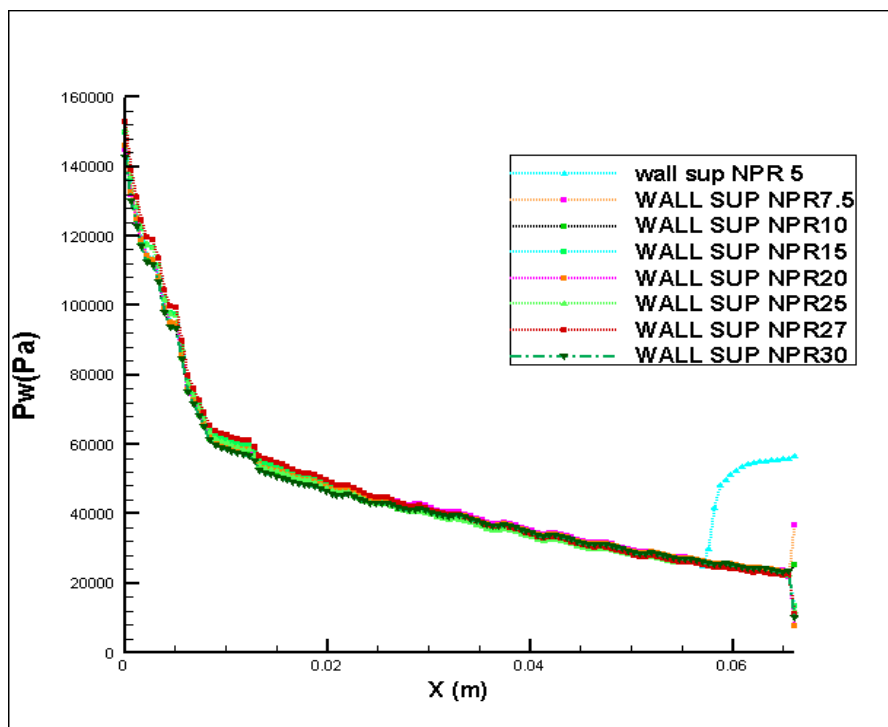


**Fig. 7.** Pressure distribution in the divergent for different NPRs

### 3.2 Effect of Fluid Injection

The detachment shock caused by the injection can, in some cases, impact the opposite wall. Its reflection can in turn take off the boundary layer. An overpressure then appears downstream of the impact point. This can significantly affect the efficiency of the thrust vectoring.



We note the presence of an oblique shock upstream of the injection slot on the upper wall. Another impact on the opposite wall close to the lip of the nozzle is due to the phenomenon of detachment caused by over-expansion and located at  $x / x_t = 0.27$  as shown in the Figure 8 and 9 (the position of the detachment corresponds to zero wall friction  $\tau_w = 0$ ). In Figure 10 and Figure 11 there is a clear deviation of the flow in the direction of the injected jet.

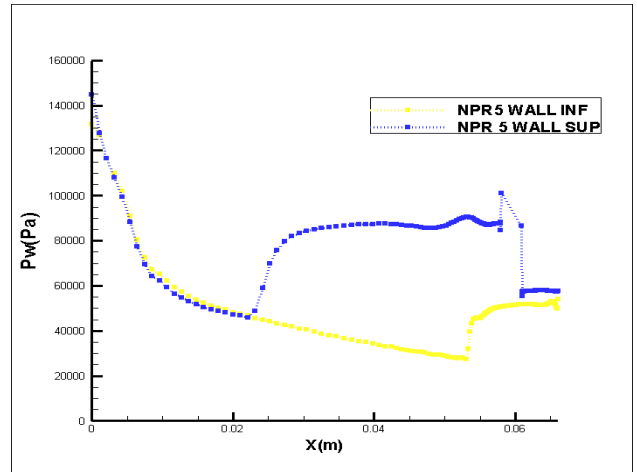
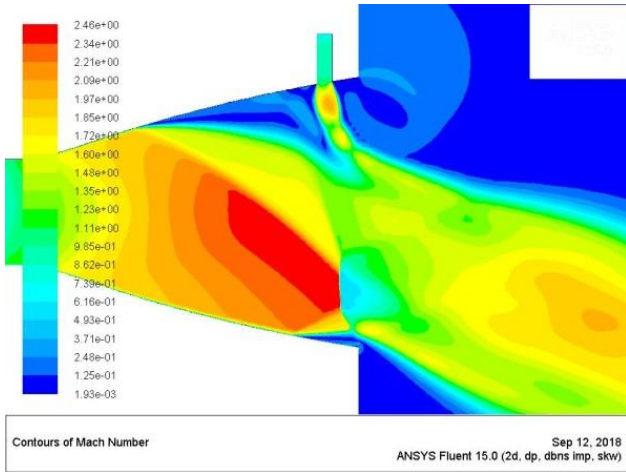


Fig. 8. Iso-Mach and pressure distribution NPR=5 and SPR=1.0

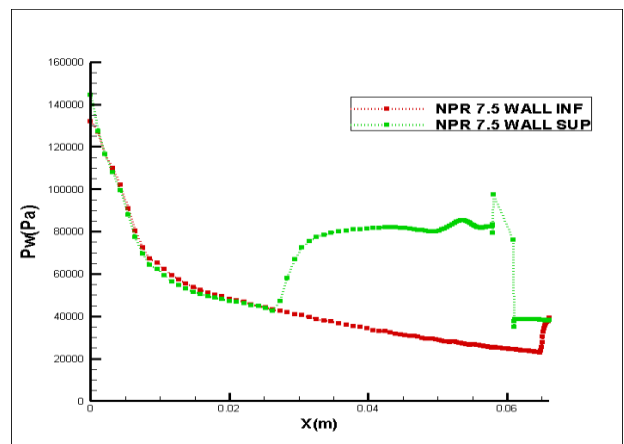
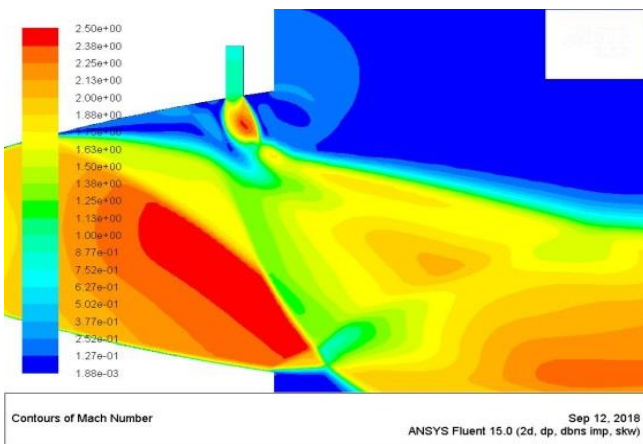


Fig. 9. Iso-Mach and pressure distribution, NPR=7.5 and SPR=1.0

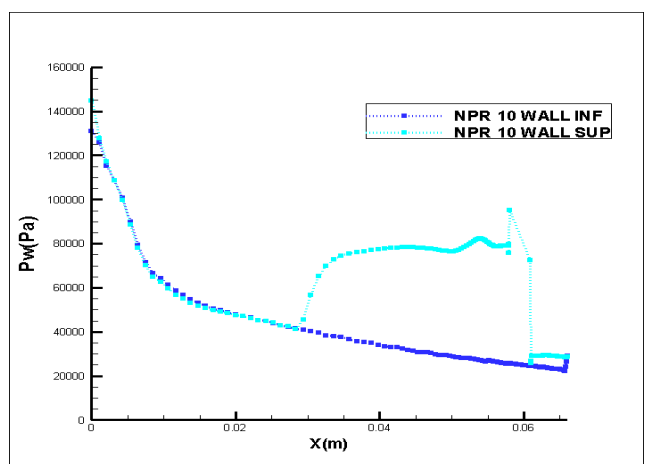
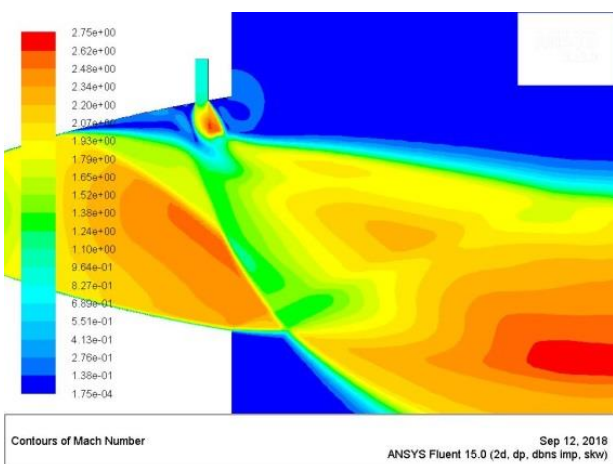
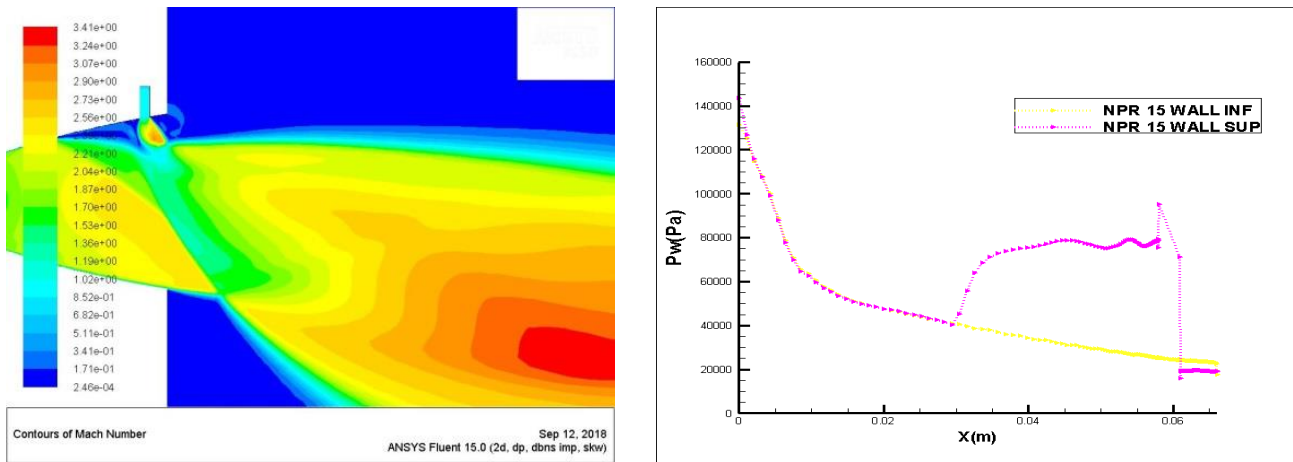


Fig. 10. Iso-Mach and pressure distribution NPR=10 and SPR=1.0



**Fig. 11.** Iso-Mach and pressure distribution, NPR=15 and SPR=1.0

Table 1 shows the results obtained by our study in comparison with those obtained by Zmijanovic [29] and the experimental results by Waithe and Deere [17]. These results are very close, which gives credibility to our study, the error between these results can be interpreted by the different approaches used by the authors.

**Table 1**  
 Comparison between our results and the experimental results for SPR = 1.0 and different NPRs

		Our results	Zmijanovic [29]	Waithe and Deere [17]
NPR = 5	$x/x_t$	3.61	3.59	3.55
	Vector angle $\delta$	$-0.7^\circ$	$-0.61^\circ$	$-0.6^\circ$
NPR = 7.5	$x/x_t$	3.21	3.2	3.1
	Vector angle $\delta$	$-0.4^\circ$	$-0.47^\circ$	$-0.55^\circ$
NPR = 10	$x/x_t$	2.99	2.9	3
	Vector angle $\delta$	$6^\circ$	$5.68^\circ$	$5.6^\circ$
NPR = 15	$x/x_t$	2.89	2.88	2.8
	Vector angle $\delta$	$8.1^\circ$	$8.08^\circ$	$8.45^\circ$
NPR = 20	$x/x_t$	2.8	2.76	2.7
	Vector angle $\delta$	$7.6^\circ$	$7.57^\circ$	$7.4^\circ$

The maximum vector angle 8.10 is obtained for an NPR equal to 15 which is very close to 8.45 and 8.08 obtained by Waithe and Deere [17] and Zmijanovic [29] respectively. Above this value of the NPR, we notice the decrease of this angle. The maximum efficiency obtained for an injection rate of 4% and an NPR equal to 15 is 2.035%, 2.02% and 2.11% respectively for our calculations, Zmijanovic [29] and the experimental by Waithe and Deere [17].

#### 4. Conclusion

The results obtained from this study showed that the thrust deflection depends on the injector pressure ratio (NPR) but also on the secondary pressure ratio (SPR). The sensitivity of the deflection is low for a large number of NPRs but becomes important in the over-expanded regime due to the increase in asymmetric forces downstream of the injector. The application made on a TIC nozzle has shown that a vector angle of 8.10 can be obtained for an NPR equal to 15 and the maximum efficiency is obtained for an injection rate of 4% is 2.035%. Our results were compared with those obtained by other authors, which gave satisfaction with a margin of error that is due

to the difference in the approaches used. Parameters such as the profile of the main nozzle, the injection conditions of the secondary and main flow have a major influence on the thrust vectoring potential of the concept. Several perspectives are envisaged for this work, such as an experimental study of injection through an annular sector, which could confirm the results obtained. Other nozzle profiles can also be studied. Supersonic injection by an annular injector can also be investigated. Finally, the in stationary aspect must also be considered. Indeed, the response time of the system could be a determining parameter in the choice of this concept.

## References

- [1] Anderson, Christopher, Victor Giuliano, and David Wing. "Investigation of hybrid fluidic/mechanical thrust vectoring for fixed-exit exhaust nozzles." In *33rd Joint Propulsion Conference and Exhibit*, p. 3148. 1997. <https://doi.org/10.2514/6.1997-3148>
- [2] Páscoa, José C., Antonio Dumas, Michele Trancossi, Paul Stewart, and Dean Vucinic. "A review of thrust-vectoring in support of a V/STOL non-moving mechanical propulsion system." *Central European Journal of Engineering* 3, no. 3 (2013): 374-388. <https://doi.org/10.2478/s13531-013-0114-9>
- [3] Maarouf, Nabegh. "Modélisation des phénomènes dissymétriques dans le divergent des tuyères supersoniques propulsives: application à la vectorisation de la poussée." *PhD diss., Evry-Val d'Essonne*, 2008.
- [4] Rosen, R., F. W. Spaid, and E. E. Zukoski. *A study of secondary injection of gases into a supersonic flow*. No. NASA-CR-76891. 1966.
- [5] Spaid, Frank William. "A study of Secondary Injection of Gases into a Supersonic Flow." *PhD diss., California Institute of Technology*, 1964. <https://doi.org/10.2514/6.1964-110>
- [6] Willard, C. M., F. J. Capone, M. Konarski, and H. L. Stevens. "Static performance of vectoring/reversing nonaxisymmetric nozzles." *Journal of Aircraft* 16, no. 2 (1979): 116-123. <https://doi.org/10.2514/3.58493>
- [7] Gallaway, C., and R. Osborn. "Aerodynamics perspective of supermaneuverability." In *3rd Applied Aerodynamics Conference*, p. 4068. 1985. <https://doi.org/10.2514/6.1985-4068>
- [8] Deere, Karen. "Computational investigation of the aerodynamic effects on fluidic thrust vectoring." In *36th AIAA/ASME/SAE/ASEE Joint Propulsion Conference and Exhibit*, p. 3598. 2000. <https://doi.org/10.2514/6.2000-3598>
- [9] Abeyounis, W. K., and B. D. Bennett Jr. "Static Internal Performance of an Over Expanded Fixed-Geometry, Nonaxisymmetric Nozzle With Fluidic Pitch-Thrust-Vectoring Capability." *NASA Paper No. TP-3645* (1997).
- [10] Flamm, Jeffrey. "Experimental study of a nozzle using fluidic counterflow for thrust vectoring." In *34th AIAA/ASME/SAE/ASEE Joint Propulsion Conference and Exhibit*, p. 3255. 1998. <https://doi.org/10.2514/6.1998-3255>
- [11] Deere, Karen. "Summary of fluidic thrust vectoring research at NASA Langley Research Center." In *21st AIAA Applied Aerodynamics Conference*, p. 3800. 2003. <https://doi.org/10.2514/6.2003-3800>
- [12] Flamm, Jeffrey, Karen Deere, Mary Mason, Bobby Berrier, and Stuart Johnson. "Experimental study of an axisymmetric dual throat fluidic thrust vectoring nozzle for supersonic aircraft application." In *43rd AIAA/ASME/SAE/ASEE Joint Propulsion Conference & Exhibit*, p. 5084. 2007. <https://doi.org/10.2514/6.2007-5084>
- [13] Miller, Daniel, Patrick Yagle, and Jeffrey Hamstra. "Fluidic throat skewing for thrust vectoring in fixed-geometry nozzles." In *37th Aerospace Sciences Meeting and Exhibit*, p. 365. 1999. <https://doi.org/10.2514/6.1999-365>
- [14] Shi, J. W., Z. X. Wang, Li Zhou, and X. L. Sun. "Investigation on flow characteristics of SVC nozzles." *Journal of Applied Fluid Mechanics* 11, no. 2 (2018): 331-342.
- [15] Shi, Jing-Wei, Zhan-Xue Wang, Zeng-Wen Liu, and Xiao-Bo Zhang. "Effects of secondary injection forms on thrust vector performance of shock vector controlling nozzle." *Journal of Aerospace Power* 28 (2013): 2678-2684.
- [16] Hunter, Craig, and Karen Deere. "Computational investigation of fluidic counterflow thrust vectoring." In *35th Joint Propulsion Conference and Exhibit*, p. 2669. 1999. <https://doi.org/10.2514/6.1999-2669>
- [17] Waithe, Kenrick, and Karen Deere. "An experimental and computational investigation of multiple injection ports in a convergent-divergent nozzle for fluidic thrust vectoring." In *21st AIAA Applied Aerodynamics Conference*, p. 3802. 2003. <https://doi.org/10.2514/6.2003-3802>
- [18] Deng, Ruoyu, Fanshi Kong, and Heuy Dong Kim. "Numerical simulation of fluidic thrust vectoring in an axisymmetric supersonic nozzle." *Journal of Mechanical Science and Technology* 28, no. 12 (2014): 4979-4987. <https://doi.org/10.1007/s12206-014-1119-x>
- [19] Chouicha, Rachid, Mohamed Sellam, and Said Bergheul. "Effect of chemical reactions on the fluidic thrust vectoring of an axisymmetric nozzle." *International Journal of Aviation, Aeronautics, and Aerospace* 6, no. 5 (2019). <https://doi.org/10.15394/ijaaa.2019.1377>

- [20] Hakim, Kbab, Hamitouche Toufik, and Bergheul Said. "Numerical Simulation of Fluidic Thrust Vectoring in The Conical Nozzle." *Journal of Advanced Research in Fluid Mechanics and Thermal Sciences* 73, no. 2 (2020): 88-105. <https://doi.org/10.37934/arfmts.73.2.88105>
- [21] Spaid, F. W., and E. E. Zukoski. "A study of the interaction of gaseous jets from transverse slots with supersonic external flows." *AIAA Journal* 6, no. 2 (1968): 205-212. <https://doi.org/10.2514/3.4479>
- [22] Ferlauto, Michele, Andrea Ferrero, Matteo Marsicovetere, and Roberto Marsilio. "Differential Throttling and Fluidic Thrust Vectoring in a Linear Aerospike." *International Journal of Turbomachinery, Propulsion and Power* 6, no. 2 (2021): 8. <https://doi.org/10.3390/ijtpp6020008>
- [23] Emelyanov, Vladislav, Mikhail Yakovchuk, and Konstantin Volkov. "Multiparameter optimization of thrust vector control with transverse injection of a supersonic underexpanded gas jet into a convergent divergent nozzle." *Energies* 14, no. 14 (2021): 4359. <https://doi.org/10.3390/en14144359>
- [24] Xue, Fei, Gu Yunsong, Yuchao Wang, and Han Qin. "Research on control effectiveness of fluidic thrust vectoring." *Science Progress* 104, no. 1 (2021): 1-17. <https://doi.org/10.1177/0036850421998137>
- [25] Chandra Sekar, T., Kundan Jaiswal, Rajat Arora, Ramraj H. Sundararaj, Abhijit Kushari, and Avijeet Acharya. "Nozzle Performance Maps for Fluidic Thrust Vectoring." *Journal of Propulsion and Power* 37, no. 2 (2021): 314-325. <https://doi.org/10.2514/1.B38044>
- [26] Song, F., L. Zhou, J. W. Shi, and Z. X. Wang. "Investigation on Flow Characteristics and Parameters Optimization of a New Concept of TC Nozzle." *Journal of Applied Fluid Mechanics* 14, no. 3 (2020): 819-832. <https://doi.org/10.47176/jafm.14.03.31908>
- [27] Chen, Jun-Lin, and Ying-Hao Liao. "Parametric Study on Thrust Vectoring with a Secondary Injection in a Convergent-Divergent Nozzle." *Journal of Aerospace Engineering* 33, no. 4 (2020): 04020020. [https://doi.org/10.1061/\(ASCE\)AS.1943-5525.0001136](https://doi.org/10.1061/(ASCE)AS.1943-5525.0001136)
- [28] Hunter, Craig A. "Experimental, Theoretical, and Computational Investigation of Separated Nozzle Flows." In *34th AIAA/ASME/SAE/ASEE Joint Propulsion Conference and Exhibit*, 1998. <https://doi.org/10.2514/6.1998-3107>
- [29] Zmijanovic, Vladeta. "Vectorisation fluidique de la poussée d'une tuyère axisymétrique supersonique par injection secondaire." *PhD diss., Orléans*, 2013.